The influence of thermal annealing on the photoconducting properties of $BaSnO_3$ films

G. Bridoux,[1, a)] J. M. Ferreyra,[1] J. Guimpel,[2] G. Nieva,[2] and M. Villafuerte[1]
[1)] *Laboratorio de Física del Sólido, INFINOA (CONICET-UNT), Facultad de Ciencias Exactas y Tecnología, Universidad Nacional de Tucumán, 4000 San Miguel de Tucumán, Argentina*
[2)] *Centro Atómico Bariloche-CNEA, Instituto Balseiro-Universidad Nacional de Cuyo and CONICET, 8400 S. C. Bariloche, Argentina*

(Dated: 29 December 2020)

Starting from high quality oxygen deficient $BaSnO_3$ films we have monitored the evolution of their electrical conducting and photoconducting properties after subsequent post-thermal annealing in oxygen. In this way, we have been able to modify the electrical conductivity of the film by at least three orders of magnitude (from 18.2 to $0.013\,\Omega^{-1}\,m^{-1}$) by simply reducing the oxygen vacancies concentration after each thermal annealing. Even though the film holds its semiconducting-like behavior, we have observed a modification of the hopping parameters concomitant with a decrease of the Fermi energy level as the electrical conductivity is reduced. Similarly, the effective energy gap extracted from photoconductance spectroscopy measurements decreases as the Fermi energy level decreases suggesting the presence of in-gap states generated by oxygen vacancies. A direct energy bulk gap value of (3.8 ± 0.1) eV was obtained. While the photoconductivity increases from $\simeq 4.6$ to 73 % its slow time constants become less dominant as the electrical conductivity is decreased in accordance with a reduction of the oxygen vacancies density which play a key role as electron-traps.

PACS numbers: 72.40.+w, 72.20.Jv

$BaSnO_3$ is a transparent wide band gap semiconductor that has attracted the attention in the last years as a possible alternative to transparent conductive oxides (TCO's) based on Indium (i.e. Indium Tin Oxide), which is a rather scarce material[1,2]. This route of research has been triggered by successful efforts to fabricate high quality $BaSnO_3$ films[3–5]. One of the most relevant properties of this material is the high electronic mobility that it can reach when it is doped with Lanthanum or Antimony[3,4,6] which is a key parameter for the development of field effect transistors[3,7–9]. Another remarkable feature of $BaSnO_3$ resides in its oxygen stability. In that regard, there is a growing number of related studies which are based on oxygen deficient films where the oxygen vacancies play an important role[10–14]. An intriguing question that arises is if these intrinsic defects can serve as electron dopants in this system[15–17] and more importantly, if there is a simple and reliable method to control these oxygen vacancies. In that regard, it is known that the study of photoconducting properties in metal transition oxides is not only appealing for optoelectronic applications[2] but it can also provide information about the role of these defects as trapping centers[18–22].

The present work offers a simple approach to tackle these questions. Starting from oxygen deficient $BaSnO_3$ films we have performed a sequence of post-thermal annealing in oxygen in order to reduce the concentration of these defects and to decrease in this way the doping of the films. After each thermal annealing, the electrical conductivity properties have been measured detecting a behavior that is in accordance with a decrease of the Fermi energy level and the doping. In addition, a tracing of the photoconducting properties shows a reduction of the effective energy gap as the Fermi energy level is decreased suggesting the presence of in-gap states generated by oxygen vacancies which also act as electron traps.

$BaSnO_3$ films were grown by pulsed laser deposition (PLD) on (001) $SrTiO_3$ (STO) substrates (dimensions: $5 \times 5 \times 0.5$ mm^3) at 700°C with an oxygen pressure of 20 mTorr using a Nd:YAG laser operated at a wavelength of 266 nm[23] with an energy density of $1.8\,J\,cm^{-2}$, a repetition rate of 10 Hz and a deposition rate of $0.06\,nm\,s^{-1}$. X-ray diffraction patterns using CuKα ($\lambda = 1.5406$ Å) show that the fabricated films grew epitaxially in the [001] direction with cubic structure, see θ-2θ scan of Fig. 1a. The resulting out-of plane lattice parameter is $a = 4.19$ Å which is slightly longer compared to the ones reported for $BaSnO_3$ single crystals ($a = 4.116$ Å)[14,24] due to an in-plane compressive strain in the film in order to match a smaller STO lattice parameter ($a = 3.91$ Å), as it was previously reported[3–5,14]. An ω-scan around the (002) reflection of $BaSnO_3$ (see inset of Fig. 1a) shows a sharp peak with a full width at half maximum (FWHM) of $\simeq 0.2°$ confirming the high texture of the fabricated films. Low angle θ-2θ scans (see Fig. 1b) show the presence of Kiessig fringes[25] which indicate that the resulting films grew with a very low surface roughness and a uniform thickness. From this latter curve a film thickness value of $d \simeq 130$ nm was estimated. Electrical conductivity and photoconductivity measurements details were described elsewhere[21,23]. In particular, for the photoconductivity measurements a standard cryostat equipped with an optical window and a 1000 W Xe lamp plus a monochromator has been employed[26]. The wavelength can be varied from 200 to 800 nm with a flux density of

[a)] Electronic mail: gbridoux@herrera.unt.edu.ar

$\sim 10\,\mu W\,cm^{-2}$ in the UV range.

A sequence of post-thermal annealing in oxygen at 500°C with $P_{O_2} = 10$ Torr and a minimum step time of 30 min were performed in the as-grown oxygen deficient film. After each thermal annealing the electrical conductivity in dark, σ_{dark}, and the photoconducting properties of the sample were measured. Fig. 1c shows how σ_{dark} of the film at room temperature decreases as the accumulated annealing time increases indicating a reduction of the oxygen vacancies concentration in the $BaSnO_3$ film and hence of its carrier density[10–13,15]. This curve can be well fitted using an exponential function with a time constant of $\tau = 1590$ s and from this value the oxygen diffusion constant for $BaSnO_3$ can be obtained via[27] $D_O = d^2/\pi^2\tau$ giving a value of $1 \times 10^{-14}\,cm^2\,s^{-1}$.

The temperature dependence of σ_{dark} in the film (in a range from 35 K to 300 K) was investigated after each thermal annealing, see Fig. 2a. As it can be observed, all the curves exhibit a semiconducting-like behavior becoming more insulating as the accumulated annealing time in oxygen increases. After a careful analysis evaluating different electrical conduction models we have found that the best expression that fits the T-dependent conductivity curves of Fig. 2a is[28,29]:

$$\sigma_{dark}(T) = \sigma_0 + \sigma_1 e^{-\epsilon_1/k_BT} + \sigma_3 e^{-\epsilon_3/k_BT} \qquad (1)$$

where ϵ_1 represents the energy required to promote an electron from the Fermi energy level, E_F, (in the proximities of a defect like an oxygen vacancy) to the conduction band, CB, see sketch of Fig. 2a. In the case of ϵ_3, which is defined as the activation energy for hopping, its interpretation has been a subject of intense debate in the last decades[28–32]. It has been interpreted as the effective energy width of the impurity band[28] but also as the energy needed to promote an electron from E_F to a defect where the density of defect states $g(E)$ is maximum[29], see sketch of Fig. 2a. From these fits, the dependence of ϵ_1 and ϵ_3 with σ_{dark} at room T can be extracted, see inset of Fig. 2b. As it is expected, ϵ_1 is higher than ϵ_3 in less than one order of magnitude[28–32]. Besides, both parameters decrease as σ_{dark} increases, suggesting an increase of the Fermi level which in turn approaches to the conduction band minimum, E_C, reducing in this way the energy required to promote an electron to it, that is ϵ_1, see sketch of Fig. 2a. On the other hand, it is known that the energy difference $E_C - E_F$ can be expressed as[33]:

$$E_C - E_F \simeq k_BT \ln(N_c\, e\mu/\sigma_{dark}) \qquad (2)$$

where N_c is the CB effective density of states ($N_c =$

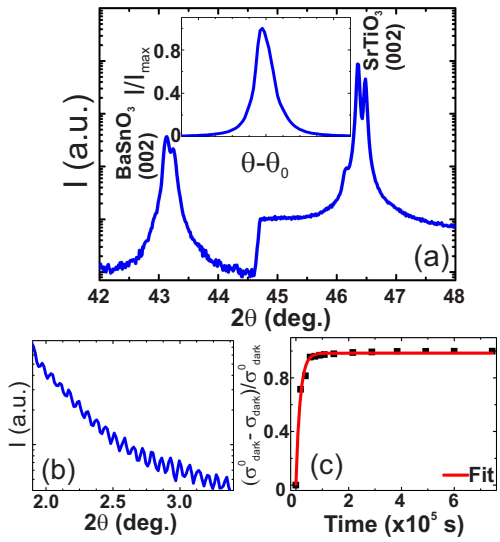

FIG. 1. (a) Typical $\theta - 2\theta$ X-ray scan of the $BaSnO_3$ film. The step like feature observed at $2\theta \simeq 44.6°$ is due to the K absorption edge of the Ni filter, which reduces the intensity of X-rays with wavelength shorter than 0.14879 nm. The inset shows an ω-scan around the (002) peak of the film. (b) Low-angle $\theta - 2\theta$ scan on the film displaying typical Kiessig fringes. (c) σ_{dark} at room T (normalized by the conductivity of the as-grown film, σ^0_{dark}) as a function of the accumulated annealing time.

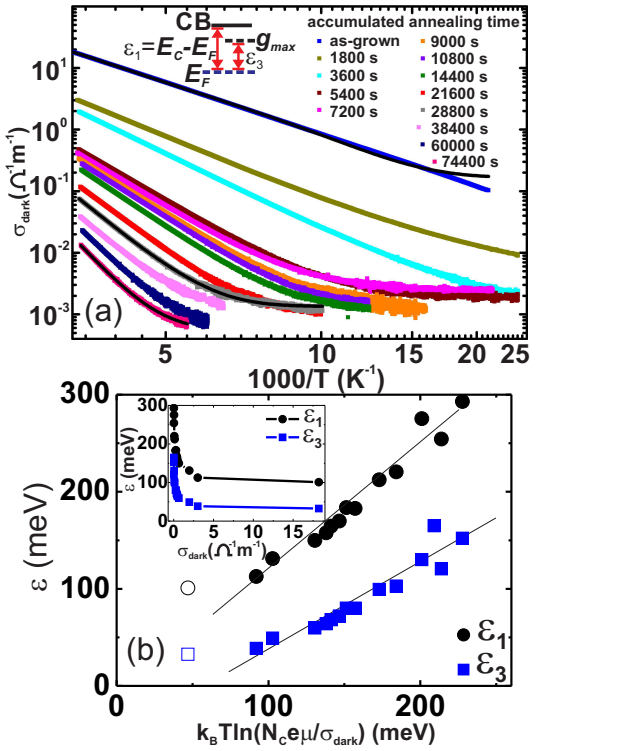

FIG. 2. (a) Temperature dependence of σ_{dark} recorded after each thermal annealing. Some of the fittings using Eq. (1) are also shown (black curves). The inset shows a sketch of the energy diagram in the proximities of the CB. (b) Extracted hopping parameters as a function of σ_{dark} at room T (inset) and $k_BT\ln(N_c\, e\mu/\sigma_{dark})$ (main panel). The empty symbols correspond to the hopping parameters for the as-grown film. The lines are guide to eyes.

$8.96\times10^{18}\,\mathrm{cm}^{-3}$ for $BaSnO_3$) and μ is the electronic mobility ($\mu \simeq 0.9\,\mathrm{cm}^2\,\mathrm{V}^{-1}\,\mathrm{s}^{-1}$, extracted from Hall effect measurements on the as-grown film) which is assumed constant. From the previous discussion, if in the plot presented in the inset of Fig. 2b the abscissa is rewritten using Eq. (2) evaluated at room T, a nearly one-to-one linear relation between ϵ_1 and Eq. (2) is obtained, see main panel of Fig. 2b. More surprisingly, a linear relation with a similar slope is also obtained for ϵ_3, see main panel of Fig. 2b. These results are in agreement with the predicted relation[29]: $\epsilon_1 \simeq E_0+\epsilon_3$ (where E_0 is the difference between E_C and the energy where $g(E)$ peaks, see sketch of Fig. 2a) and also with the interpretation that a decrease of $E_C - E_F$ due to an increase of both σ_{dark} and E_F will lead to a reduced ϵ_3, see sketch of Fig. 2a.

Photoconductance spectroscopy measurements at room T were performed in the film after each thermal annealing, typical spectrum is shown in Fig. 3a. In a first approximation, the photoconductivity, PC, (defined as $PC = (\sigma - \sigma_{dark})/\sigma_{dark}$) can be assumed to be proportional to the optical absorption coefficient in the proximities of the onset[23]. In addition, since $BaSnO_3$ has a direct energy bulk gap[6,11,15,34–40], E_G^{bulk}, the effective energy gap, E_G, can be extracted assuming that the relation $PC^2 \propto E - E_G$ holds in a certain range of energies, see Fig. 3a. In contrast to E_G^{bulk}, which represents a band to band transition, E_G is an optoelectronic gap defined as the energy needed to promote a photoelectron from the valence band, VB, to a state where it can conduct, see sketch of Fig. 3b. The inset of Fig. 3a shows how the extracted E_G increases and then it tends to saturate at $E_G \simeq 3.7\,\mathrm{eV}$ when σ_{dark} at room T is increased. Since it would be expected that E_G increases as both σ_{dark} and E_F increase approaching E_C (see sketch of Fig. 3b) it is reasonable to plot the curve of the inset of Fig. 3a using again Eq. (2) as abscissa. The results are summarized in the main panel of Fig. 3c. As it can be observed, a linear relation between E_G and Eq. (2) is obtained, confirming the linear increase of E_G as $E_C - E_F$ decreases, see sketch of Fig. 3b. According to this and taking into account that $\epsilon_1 \sim E_C - E_F$, the relation $E_G^{bulk} \simeq \epsilon_1 + E_G$ should be satisfied for all σ_{dark} values with the same value of E_G^{bulk}, see sketch of Fig. 3b. Using the ϵ_1 and E_G values of Fig. 2b and Fig. 3c respectively we have obtained a con-

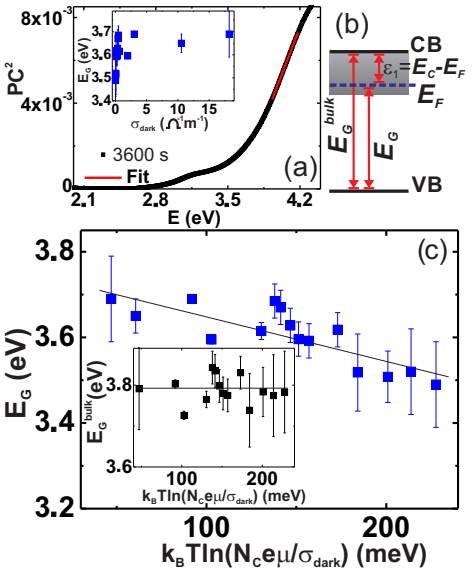

FIG. 3. (a) Typical PC^2 spectrum and its corresponding linear fit at room T for an accumulated annealing time of 3600 s. The inset shows the extracted E_G values as a function of σ_{dark} at room T. (b) Energy diagram sketch. (c) E_G as a function of $k_BT\ln(N_c\,e\mu/\sigma_{dark})$. The inset shows $E_G^{bulk} \simeq \epsilon_1 + E_G$ as a function of $k_BT\ln(N_c\,e\mu/\sigma_{dark})$. The lines are guide to eyes.

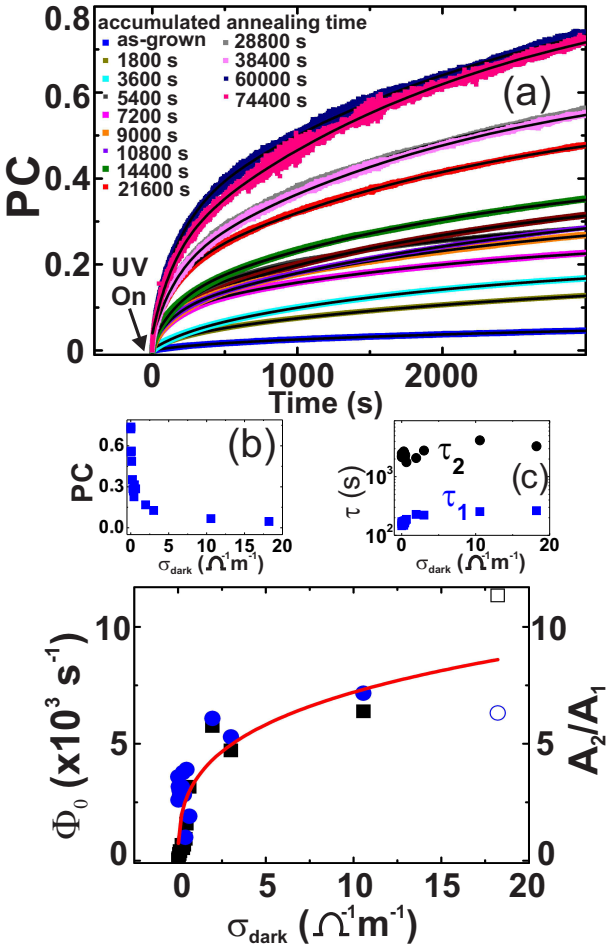

FIG. 4. (a) PC as a function of time under UV illumination at room T. Each curve was recorded after each thermal annealing. The employed incident light energy was close to E_G. The corresponding fittings using Eq. (3) are also shown (black curves). Extracted PC saturation values (b) and time constants (c) as a function of σ_{dark} at room T. (d) σ_{dark} dependence of Φ_0 (black squares, left axis) and A_2/A_1 (blue circles, right axis). A fit using Eq. (5) is also shown (red curve). The empty symbols correspond to the parameters for the as-grown film.

stant E_G^{bulk} value of (3.8±0.1) eV, see inset of Fig. 3c. The wide dispersion in the literature values of E_G^{bulk}, which range between $\simeq$ 3.1 and 4.0 eV[6,11,15,34–40], may be due to the fact that actually E_G is being reported.

This picture implies the presence of a high density of defect states (i.e. due to oxygen vacancies) or an hybridization between these states and the CB resulting in a band tail within the band gap[41,42], see sketch of Fig. 3b. The latter scenario has already been proposed in $BaSnO_3$[8].

Time dependent photoconductivity measurements at room T were carried out in the film after each thermal annealing, the results being summarized in Fig. 4a. Photoconductivity with values ranging from $\simeq$ 4.6 to 73 % was observed, with a higher PC for lower values of σ_{dark}, see Fig. 4b. The time dependent curves of Fig. 4a can be well fitted by the sum of two exponential functions[18,19]:

$$PC = y_0 + A_1 e^{-t/\tau_1} + A_2 e^{-t/\tau_2} \quad (3)$$

where τ_1 and τ_2 are a fast and slow time constants respectively. Their resulting values for each σ_{dark} value are summarized in Fig. 4c. As it can be observed, these time constants do not vary with σ_{dark}. Each exponential term represents a certain type of carrier trap where the weight factors A_1 and A_2 are related to their corresponding concentration[19]. The σ_{dark} dependence of the ratio A_2/A_1 is presented in Fig. 4d (blue circles, right axis). As it can be observed, after a sharp increase at low σ_{dark} values, A_2/A_1 slowly tends to a saturation as σ_{dark} is increased, suggesting that the concentration of traps of the type 2 grows with σ_{dark}. Since an increase of σ_{dark} is related to a growth of the oxygen vacancies concentration, the type 2 traps can be associated to these electron trap defects[15]. On the other hand, the behavior observed in Fig. 4b can be explained using the following phenomenological expression that relates PC and σ_{dark}[26,43]:

$$PC = \frac{e\,\mu\,\eta\,\Phi\,\tau'}{\sigma_{dark}\,A\,l(1+(\Phi/\Phi_0)^n)} \quad (4)$$

where Φ is the photon absorption rate, η is the quantum efficiency and Φ_0 is the photon absorption rate when trap saturation occurs. A and l are the cross section and the length of the film respectively. τ' is the photoelectron carrier lifetime associated with the most efficient type of traps centers. Hence it is plausible to assume that $\tau' \simeq \tau_2$. Taking $n = 0.7$ and assuming that $\eta \simeq 1$[26,43] the σ_{dark} dependence of Φ_0 can be extracted (black squares, left axis of Fig. 4d). At first glance, Φ_0 follows a similar dependence to that of A_2/A_1 which is a logical result considering that Φ_0 is related to a trap concentration associated to the slow time response τ_2. The dependence observed in Fig. 4d involves not only the growth of oxygen vacancies concentration as σ_{dark} is increased but also the loss of efficiency of these electron traps as they become occupied as σ_{dark} increases and E_F approaches E_C, see sketch of Fig. 3b. From these arguments, we propose that the concentration of these empty traps is proportional to $\int_{E_F}^{E_C} g(E,\sigma_{dark})dE$ with a density of defect states $g(E,\sigma_{dark})$ that grows with σ_{dark}. That is: $g(E,\sigma_{dark}) \simeq N(\sigma_{dark})\,G(E)$ with $N(\sigma_{dark}) = \alpha\,\sigma_{dark}^{\beta}$, where α and β are fitting parameters. Evaluating the latter integral we get: $\int_{E_F}^{E_C} g(E,\sigma_{dark})dE = N(\sigma_{dark})(\bar{G}(E_C) - \bar{G}(E_F))$ where $\bar{G}(E)$ is the primitive function of $G(E)$. Performing a Taylor series expansion of $\bar{G}(E_F)$ at E_C and keeping the first order terms we obtain: $\int_{E_F}^{E_C} g(E,\sigma_{dark})dE = \alpha\,\sigma_{dark}^{\beta} G(E_C)(E_C - E_F)$. Finally, using Eq. (2), the latter integral can be written as:

$$A_2/A_1 \simeq \int_{E_F}^{E_C} g(E)dE = \alpha_1\,\sigma_{dark}^{\beta}\ln(N_c\,e\mu/\sigma_{dark}) \quad (5)$$

where $\alpha_1 = \alpha\,k_B T\,G(E_C)$. As it can be observed, the data of Fig. 4d can be well fitted using Eq. (5) with a β value of 0.4 supporting in this way the proposed scenario.

In summary, the electrical conducting and photoconducting properties of oxygen deficient $BaSnO_3$ films have been gradually monitored as subsequent post-thermal annealing in oxygen have been performed. The increment of the hopping parameters and the reduction of the E_G values as the film is oxygenated responds to a reduction of E_F and of the donor doping with oxygen vacancies. These defects also play a relevant role as electron traps in the observed photoconductivity.

This work was supported by PIP- No. 585, SCAIT- No. E653CX, PICT- No. 2016-3356 , SNMAG and SINALA facilities.

[1] C. A. Hoel, T. O. Mason, J. -F. Gaillard and K. R. Poeppelmeier, Chem. Mater. **22**, 3569 (2010).
[2] X. Yu, T. J. Marks and A. Facchetti, Nat. Mater. **15**, 383 (2016).
[3] U. Kim, C. Park, T. Ha, R. Kim and H. S. Mun, H. M. Kim, H. J. Kim, T. H. Kim, N. Kim, J. Yu, K. H. Kim, J. H. Kim and K. Char, APL Mater. **2**, 056107 (2014).
[4] U. Kim, C. Park, T. Ha, Y. M. Kim, N. Kim, C. Ju, J. Park, J. Yu, J. H. Kim and K. Char, APL Mater. **3**, 036101 (2015).
[5] S. Raghavan, T. Schumann, H. Kim, J. Y. Zhang, T. A. Cain and S. Stemmer, APL Mater. **4**, 016106 (2016).
[6] H. F. Wang, Q. Z. Liu, F. Chen, G. Y. Gao, W. Wu and X. H. Chen, J. Appl. Phys. **101**, 106105 (2007).
[7] J. Shin, Y. M. Kim, Y. Kim, C. Park and K. Char, Appl. Phys. Lett. **109**, 262102 (2016).
[8] A. V. Sanchela, T. Onozato, B. Feng, Y. Ikuhara and H. Ohta, Phys. Rev. Mat. **1**, 034603 (2017).
[9] J. Park, H. Paik, K. Nomoto, K. Lee, B. -E. Park, B. Grisafe, L. -C. Wang, S. Salahuddin, S. Datta, Y. Kim, D. Jena, H. G. Xing and D. G. Schlom, APL Mater. **8**, 011110 (2020).
[10] W. -J. Lee, H. J. Kim, E. Sohn, H. M. Kim, T. H. Kim, K. Char, J. H. Kim and K. H. Kim, Phys. Status Solidi A **212**, 1487 (2015).
[11] Q. Liu, J. Dai, Y. Zhang, H. Li, B. Li, Z. Liu and W. Wang, J. Alloys and Compounds **655**, 389 (2016).
[12] H. M. Iftekhar Jaim, S. Lee, X. Zhang and I. Takeuch, Appl. Phys. Lett. **111**, 172102 (2017).
[13] B. Luo and J. Hu, ACS Electr. Mater. **1**, 51 (2019).

[14]H. J. Kim, U. Kim, H. M. Kim, T. H. Kim, H. S. Mun, B. -G. Jeon, K. T. Hong, W. -J. Lee, C. Ju and K. H. Kim, Appl. Phys. Express **5**, 061102 (2012).
[15]D. O. Scanlon, Phys. Rev. B **87**, 161201(R) (2013).
[16]L. Weston, L. Bjaalie, K. Krishnaswamy and C. G. Van de Walle, Phys. Rev. B **97**, 054112 (2018).
[17]J. Buckeridge, C. R. A. Catlow, M. R. Farrow, A. J. Logsdail, D. O. Scanlon, T. W. Keal, P. Sherwood, S. M. Woodley, A. A. Sokol and A. Walsh, Phys Rev. Mat. **2**, 054604 (2018).
[18]R. H. Bube, *Photoelectronics Properties of Semiconductors*, (Cambridge University Press, Cambridge, 1992).
[19]S. A. Studenikin, N. Golego and M. Cocivera, J. Appl. Phys. **83**, 2104 (1998).
[20]M. C. Tarun, F. A. Selim and M. D. McCluskey, Phys. Rev. Lett. **111**, 187403 (2013).
[21]G. Bridoux, M. Villafuerte, J. M. Ferreyra, N. Bachi, C. A. Figueroa and S. P. Heluani, Phys. Rev. B **92**, 155202 (2015).
[22]J. M. Ferreyra, G. Bridoux, M. Villafuerte, B. Straube, J. Zamora, C. A. Figueroa and S. P. Heluani, Sol. State Commun. **257** 42 (2017).
[23]G. Bridoux, M. Villafuerte, J. M. Ferreyra, J. Guimpel, G. Nieva, C. A. Figueroa, B. Straube and S. P. Heluani, Appl. Phys. Lett. **112**, 092101 (2018).
[24]H. M. Park, H. J. Lee, S. H. Park and H. I. Yoo, Acta Crystallogr., Sect. C: Cryst. Struct. Commun. **59**, i131-i132 (2003).
[25]H. Kiessig, Ann. Phys. **402**, 769 (1931).
[26]M. Villafuerte, D. J. Zamora, G. Bridoux, J. M. Ferreyra, M. Meyer and S. P. Heluani, J. Appl. Phys. **121**, 064501 (2017).
[27]L. Malavasi and G. Flor, J. Phys. Chem. B **107**, 13880 (2003).
[28]N. Mott and E. Davis, *Electronic Processes in Non-Crystalline Materials*, 2nd ed. (University Press, Oxford, 1979).
[29]B. Shklovskii and A. Efros, *Electronic Properties of Doped Semiconductors*, Solid-State Science Vol. 45 (Springer-Verlag, 1984).
[30]H. Fritzsche, J. Phys. Chem. Solids **6**, 69 (1958).
[31]A. Miller and E. Abrahams, Phys. Rev. **120**, 745 (1960).
[32]M. Ortuno and M. Pollak, J. Phys. C: Solid State Phys. **16** 1459 (1983).
[33]R. Heinhold, G. T. Williams, S. P. Cooil, D. A. Evans and M. W. Allen, Phys. Rev. B **88**, 235315 (2013).
[34]R. J. Cava, P. Gammel, B. Batlogg, J. J. Krajewski, W. F. Peck, Jr., L. W. Rupp, Jr., R. Felder and R. B. van Dover, Phys. Rev. B **42**, 4815 (1990).
[35]H. Mizoguchi, H. W. Eng and P. M. Woodward, Inorg. Chem. **43**, 1667 (2004).
[36]X. Luo, Y. S. Oh, A. Sirenko, P. Gao, T. A. Tyson, K. Char and S.-W. Cheong, Appl. Phys. Lett. **100**, 172112 (2012).
[37]H. J. Kim, U. Kim, T. H. Kim, J. Kim, H. M. Kim, B. -G. Jeon, W. -J. Lee, H. S. Mun, K. T. Hong, J. Yu, K. Char and K. H. Kim, Phys. Rev. B **86**, 165205 (2012).
[38]H. J. Kim, J. Kim, T. H. Kim, W.-J. Lee, B. -G. Jeon, J. -Y. Park, W. S. Choi, D. W. Jeong, S. H. Lee, J. Yu, T. W. Noh and K. H. Kim, Phys. Rev. B **88**, 125204 (2013).
[39]S. A. Chambers, T. C. Kaspar, A. Prakash, G. Haugstad and B. Jalan, Appl. Phys. Lett. **108**, 152104 (2016).
[40]T. Schumann, S. Raghavan, K. Ahadi, H. Kim and S. Stemmer, J. Vac. Sci. Technol. A **34**, 050601 (2016).
[41]N. Shanthi and D. D. Sarma, Phys. Rev. B **57**, 2153 (1998).
[42]Y. Ishida, R. Eguchi, M. Matsunami, K. Horiba, M. Taguchi, A. Chainani, Y. Senba, H. Ohashi, H. Ohta and S. Shin, Phys. Rev. Lett. **100**, 056401 (2008).
[43]C. Soci, A. Zhang, B. Xiang, S. Dayeh, D. Aplin, J. Park, X. Bao, Y. Lo, and D. Wang, Nano Letters **7**, 1003 (2007).